GAIA: TRAJECTORY DESIGN WITH TIGHTENING CONSTRAINTS

Florian Renk[(1)] **and Markus Landgraf**[(2)]
[(1)(2)]*European Space Operations Center, European Space Agency, Robert-Bosch-Str. 5, 64293 Darmstadt, Germany, +49-6151-90-2443, Florian.Renk@esa.int / Markus.Landgraf@esa.int*

Abstract: *Gaia is the European Space Agency's successor mission to Hipparcos with the primary science objective to survey one billion stars in our galaxy and local galactic neighbourhood in order to build a 3D map of the Milky Way one hundred times more precise than earlier efforts. The operational orbit of Gaia is a small amplitude Lissajous orbit about the night side Sun-Earth Libration Point. The paper will describe the evolution of the mission analysis work performed to deliver Gaia safely into its operational orbit covering the launch, transfer and operation phases. This work was undertaken under the special aspect of evolving constraints during the design phase and additional constraints that surfaced after the spacecraft had already been constructed as e.g. incorrect propellant allocation on the spacecraft and a predicted high directional manoeuvre execution error. It will also introduce the mitigation strategies implemented to recover a sufficiently large launch window for a launch in the fourth quarter of 2013.*

Keywords: *Gaia, Libration Point, Lagrange Point, Mission Analysis, Mission Design*

1. Introduction

Gaia's primary objective is to survey one thousand million (one billion) stars in our galaxy and local galactic neighbourhood in order to build the most precise 3D map of the Milky Way and answer questions about its origin and evolution. The mission's secondary objectives reveal Gaia as the ultimate discovery machine. It is expected to find up to ten thousand planets beyond our Solar System and hundreds of thousands of asteroids and comets within it. The mission will also reveal tens of thousands of failed stars and supernovae, and will even test Einstein's famous theory of General Relativity.

This paper first introduces the baseline mission design of Gaia, which is a transfer and operation on a small amplitude Lissajous orbit about the Sun-Earth Libration Point 2. A general introduction to libration point orbits will be given first, followed by a discussion on the operational orbit of Gaia. Then the required mission steps from launch to disposal will be discussed for the Gaia trajectory design and the nominal constraints on the trajectory design resulting from the Gaia spacecraft (S/C) design, e.g. unavailability of omnidirectional thrust, will be introduced. In the following section the two issues resulting from incorrect manoeuvre efficiency calculation and unexpectedly large manoeuvre execution errors will be presented. The required mitigation strategies are described, detailing how the new constraints could be accommodated into the trajectory design to avoid other expensive options.

The information provided in this paper shall help to avoid similar problems for future mission by raising the awareness for these issues.

2. Libration Point Orbits

Libration points exist in a system of two massive celestial bodies orbiting each other. These bodies are referred to as the primaries or primary and secondary, with the larger and smaller mass, respectively. This section gives an introduction to the motion in the vicinity of a libration point orbit. A more detailed analysis can be found in [1, 2]. As an approximation of the real system we use the circular restricted three-body problem (CR3BP), assuming that the primary and secondary body are on circular orbits. The rotating coordinate frame, having its origin in the barycenter of the two bodies, is defined with the x-axis pointing from the primary body to the secondary, e.g. the Sun to the Earth, the z-axis pointing in the direction of the orbit normal and the y-axis supplementing the system to be a right hand one. The well known equation of motion of a third massless body in the CR3BP [3, 4] can be written as

$$\begin{aligned} \ddot{x} - 2\dot{y} &= U_x, \\ \ddot{y} + 2\dot{x} &= U_y, \\ \ddot{x} &= U_z. \end{aligned} \tag{1}$$

The distances and velocities are normalized by the distance between the primaries and their angular velocity, respectively, and the effective potential U is:

$$U = \frac{1-\mu}{r_1} + \frac{\mu}{r_2} + \frac{1}{2}(x^2 + y^2) \tag{2}$$

with $\mu = \frac{m_2}{m_1+m_2}$ and m_1, r_1 and m_2, r_2 being the masses and distance of the S/C from primary and secondary, respectively. The general solution for the collinear points can then be written as

$$\begin{aligned} x =& A_1 e^{\lambda_{xy}} + A_2 e^{-\lambda_{xy}} + A_3 \cos \omega_{xy} t + A_4 \sin \omega_{xy} t, \\ y =& c_1 A_1 e^{\lambda_{xy}} - c_1 A_2 e^{-\lambda_{xy}} + c_2 A_4 \cos \omega_{xy} t - c_2 A_3 \sin \omega_{xy} t, \\ z =& A_z \cos(\omega_z t + \Phi_z) \end{aligned} \tag{3}$$

with the constants c_1, c_2, λ_{xy}, λ_z, ω_{xy} and ω_x solely depending on the mass parameter μ and the integration constants A_1, A_2, A_3, A_4 and Φ_z depending on the initial conditions of the system.

This solution gives a good idea of the motion of a libration point orbit and also about a transfer strategy. The initial conditions $\vec{x}_0$ can be selected in such a way that only the oscillatory mode with the amplitudes A_3, A_4 and A_z are excited. The exponential terms are then not involved in the solution and we have two oscillations with slightly different frequencies, one in the xy-plane and one in the z-direction. For the in- and out-of-plane motion the amplitudes A_x, $A_y = c_2 A_x$ and A_z can be calculated. The resulting trajectory in the rotating frame is a Lissajous figure, hence, these orbits are called Lissajous orbits. The two exponential terms, represented by the so called stable and unstable amplitudes A_2 and A_1, can be associated with the so called "stable" and "unstable" manifolds, which are "tubes" in space leading to, or departing from the libration point orbit. In the case of the Sun-Earth system, initial conditions close to Earth can be found where only the oscillatory mode and the exponentially decreasing term are excited. The S/C will then travel towards the libration point orbit on the tube of the stable manifold, resulting in a so called "free-transfer"-trajectory, since due to the decreasing exponential component the motion of the S/C will eventually be dominated by the oscillatory modes without further manoeuvres [5]. In the case of the Earth-Moon system such initial conditions do not exist. Some of the manifolds do again approach the secondary body (Moon), but not the primary body (Earth). The transfer trajectory options are discussed in [6].

The solution to the equations of motion as provided in Equations 3 is based on the linearized equations of motion of the CR3BP and is therefore only valid in the vicinity of the associated libration point. For large libration point orbit amplitudes the non-linear effects will have to be taken into account. Since a numerical propagation in a realistic system, e.g. taking the eccentricity and third body perturbations into account, will always deviate from this solution, a set of "osculating Lissajous elements" [A_1, A_2, A_x, A_z, Φ_{xy}, Φ_z] can be defined similar to the "osculating Kepler elements" [7]. The following relationship allows for their calculation at a given epoch (setting $t = 0$):

$$\begin{aligned}
x =& A_1 e^{\lambda_{xy} t} + A_2 e^{-\lambda_{xy} t} + A_x \cos\left(\omega_{xy} t + \Phi_{xy}\right), \\
y =& c_1 A_1 e^{\lambda_{xy} t} - c_1 A_2 e^{-\lambda_{xy} t} - c_2 A_x \sin\left(\omega_{xy} t + \Phi_{xy}\right), \\
z =& A_z \cos\left(\omega_z t + \Phi_z\right), \\
\dot{x} =& A_1 \lambda_{xy} e^{\lambda_{xy} t} - A_2 \lambda_{xy} e^{-\lambda_{xy} t} - A_x \omega_{xy} \sin\left(\omega_{xy} t + \Phi_{xy}\right), \\
\dot{y} =& c_1 A_1 \lambda_{xy} e^{\lambda_{xy} t} + c_1 A_2 \lambda_{xy} e^{-\lambda_{xy} t} - c_2 A_x \omega_{xy} \cos\left(\omega_{xy} t + \Phi_{xy}\right), \\
\dot{z} =& - A_z \omega_z \sin\left(\omega_z t + \Phi_z\right).
\end{aligned} \tag{4}$$

Perturbations on the trajectory will always cause a small A_1 component to exist, making the collinear libration point orbits unstable.

2.1. Escape and Non-escape Direction in the Linear Problem

Assuming a manoeuvre $\Delta\vec{v} = (\Delta\dot{x}_0, \Delta\dot{y}_0, 0)$ in the xy-plane is executed at a point $\vec{x}_0 = (x_0, y_0, z_0, \dot{x}_0, \dot{y}_0, \dot{z}_0)$ on a libration point orbit results in the new amplitudes $\hat{A}_1$ and $\hat{A}_2$ [7]:

$$\begin{pmatrix} \hat{A}_1 \\ \hat{A}_2 \end{pmatrix} = \begin{pmatrix} \frac{c_2 \omega_x y}{2d_1} & \frac{\omega_{xy}}{2d_2} & -\frac{c_2}{2d_2} & \frac{1}{2d_1} \\ \frac{c_2 \omega_x y}{2d_1} & -\frac{\omega_{xy}}{2d_2} & \frac{c_2}{2d_2} & \frac{1}{2d_1} \end{pmatrix} \begin{pmatrix} x_0 \\ y_0 \\ \dot{x}_0 + \Delta\dot{x}_0 \\ \dot{y}_0 + \Delta\dot{y}_0 \end{pmatrix}. \tag{5}$$

Starting from a state vector $\vec{x}_0$ which satisfies $A_1 = 0$, any velocity increment $\Delta\vec{v} = \left(\Delta\dot{x}_0, \dot{\Delta y}_0\right)$ in the xy-plane which satisfies $\vec{u}^T \Delta\vec{v} = 0$ with

$$\vec{u} = \begin{pmatrix} -\frac{c_2}{d_2} \\ \frac{1}{d_1} \end{pmatrix} \tag{6}$$

will not lead to an escape from the family of orbits with periodic components only. $\hat{A}_1$ remains zero and the $\hat{A}_2$ component will exponentially decay. The periodic z-motion remains unaffected. The vector $\vec{u}$ defines the **escape direction** while the vector

$$\vec{s} = \begin{pmatrix} \frac{1}{d_1} \\ \frac{c_2}{d_2} \end{pmatrix} \tag{7}$$

in the xy-plane orthogonal to $\vec{u}$ defines the **non-escape direction**.

The escape direction is important for the numerical construction of non-escape orbits about the collinear libration points, while the non-escape direction is important for manoeuvres changing the amplitude of the orbit as well as eclipse and occultation avoidance.

2.2. Classification of Libration Point Orbits

To investigate transfer trajectories it is of course important to know the final conditions at the destination. It is not sufficient to just specify an arbitrary libration point orbit as destination, since several different types of orbits with specific properties exist. These orbits will deviate significantly from the linear solution derived in Equation 3, but the osculating Lissajous elements as defined in Equation 4 still remain meaningful, even for orbits with a large deviation from the solution of the linearized equations of motion. From literature [8] four different kinds of orbits are known to exist in the Sun-Earth and the Earth-Moon system. In the scope of this work they are defined as follows:

Lyapunov Orbits are planar orbits that have no out-of-plane motion and that entirely lie in the orbital plane of the primaries.

Lissajous Orbits are defined to be orbits with an in- and out-of-plane oscillation. However, the frequencies of the oscillation of the in- and out-of-plane motion differ. Lissajous orbits can be seen as quasi-symmetric to the xy-plane and the xz-plane.

Halo Orbits also have an in- and out-of-plane motion, but here the frequencies are equal and therefore the orbits are periodic. The symmetry to the xy-plane of the primaries does not exist anymore. Halo orbits only exist for a minimum in-plane amplitude and provide an exclusion zone about the line connecting the primaries.

Quasi-Halo Orbits are a ”mixture” of Lissajous and Halo orbits. Quasi-Halo orbits originate from Lissajous orbits from a certain minimum boundary value of the out-of-plane amplitude. At this boundary amplitude the Lissajous orbits loose their symmetry with respect to the *xy*-plane and start to develop an exclusion zone about the line connecting the primaries.

3. Gaia Orbit Selection and Basic Transfer Consideration

Gaia has been designed as a spinning S/C. The stars projected on the focal plane are passing over different detectors located in the focal plane and are then positioned and characterized. Due to its design as a spinning S/C and the specific attitude of Gaia required for the selected scan law the position of the Earth varies significantly when seen in the S/C reference frame. The excursion of the Earth in the S/C frame depends on the size of the libration point orbit. The limitation of the phased array antenna (PAA) installed together with the attitude strategy of Gaia enforced a maximum Sun-S/C-Earth angle (SSCE) of 15°, which is limiting the amplitudes of the libration point orbit below the ones accessible from Earth via a free transfer trajectory. The stable manifold of small amplitude Lissajous orbits does not have an intersection with the near-Earth environment. This is shown in Fig. 1, which depicts the operational orbit of Gaia together with the associated stable manifold. No part of the stable manifold intersects with the Earth.

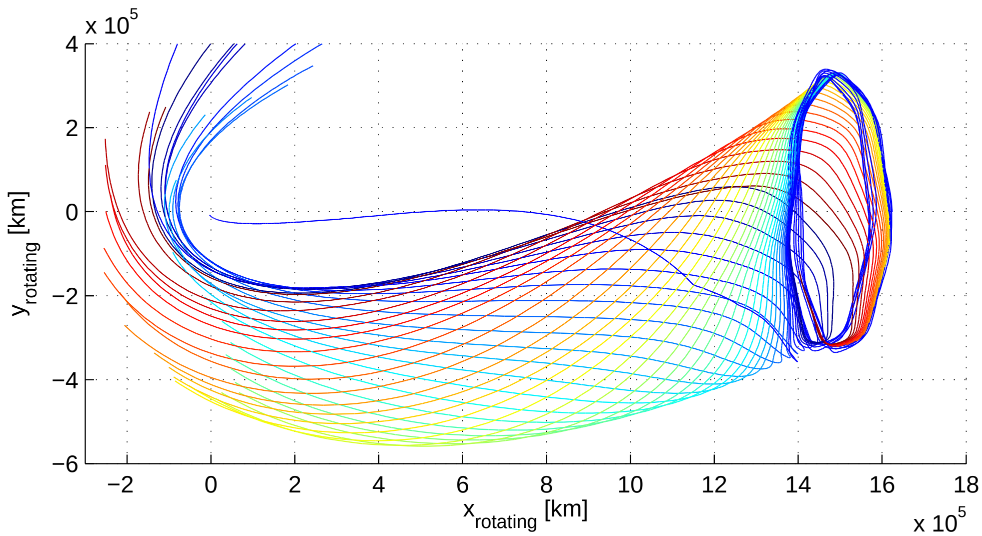

Figure 1. Stable Manifold of Gaia operational orbit and transfer trajectory. The Earth is located at the origin. Manoeuvres in the transfer trajectory are required to achieve an insertion of Gaia onto the stable manifold.

In general two different transfer options towards such a Lissajous orbit exist. Two local minima in the ΔV optimization are possible, the slow and fast transfer. The slow transfer option has the advantage of slightly less ΔV requirements, however, the Sun-S/C-Earth angle constraint is violated during the transfer phase and can be problematic for communications. Thus operations during the commissioning or science phase would be restricted. The fast transfer is slightly more expensive in terms of ΔV, however, the operational orbit is reached after about one month after the execution of the amplitude reduction manoeuvre. For Gaia the fast transfer option was selected. The two insertion manoeuvres of Gaia can also be seen in Figure 1 at about $x_{rotating} = 11 \cdot 10^5 km$, where the transfer trajectory originating from the Earth shows as distinct bend. This is followed by a second manoeuvre, at about $x_{rotating} = 12.5 \cdot 10^5 km$, after which the trajectory is on the stable manifold, its projection parallels the lines representing the stable manifold.

Small amplitude Lissajous orbits with a SSCE angle limit of 15° have the disadvantage of eclipses. The maximum eclipse free period on such an orbit is about 6.5 years after which an eclipse will occur, caused by the beat frequency of the in- and out-of-plane oscillation (compare Equ. 4). An eclipse avoidance manoeuvre can be executed to achieve another eclipse free cycle. With a nominal science period of 5 years and a commissioning period of 6 months an insertion into a Lissajous orbit being eclipse free for 5.5 years was planned. The possible mission extension of 1 year was not considered for the insertion onto the operational orbit. The insertion manoeuvre of Gaia thus served three different purposes: Reduction of in-plane amplitude, reduction of out-of-plane amplitude and adjustment of the out-of-plane phase angle for an eclipse free nominal science phase.

To cope with the inherent instability of collinear Sun-Earth libration point orbits station-keeping manoeuvres to remove the unstable component from the motion were planned every 30 days.

The basic transfer and operational strategy consisted of the following steps:

- Launch into a close to parabolic elliptical orbit (apogee about $1 \cdot 10^6$ km)
- First correction manoeuvre 1-2 days after launch to remove launcher dispersion and adjust apogee altitude due to lunar perturbation. If beneficial also the out-of-plane velocity is adjusted to benefit from vector addition effects.
- Second and third correction manoeuvre to target insertion point
- Execution of insertion manoeuvre 18-30 days after launch (fast transfer)
- Regular station-keeping manoeuvre
- Optional: Moon eclipse duration reduction manoeuvre
- Optional: Earth eclipse avoidance for mission extension
- Disposal

The launch of Gaia was planned on a Soyuz-Fregat rocket out of ESA's spaceport in Kourou, French Guiana. One possibility to launch toward a libration point orbit is the maximum payload launch into an orbit with close to parabolic velocity utilizing a direct ascent trajectory. The resulting separation orbit has an inclination of 5-6° and a fixed argument of perigee. This inclination is with respect to the Earth's equator, which is tilted 23.5° with respect to the ecliptic plane. The combination of inclination, argument of perigee and Earth's axis tilt can lead to an unfavourable geometric situation. Since the line-of-apsides must point into the direction of SEL2, the out-of-ecliptic plane component of the line-of-apsides vector can become rather large over one year. A large out-of-plane component results in a large out-of-plane amplitude, which needs to be reduced to achieve the small SSCE angle. Since this reduction is costly in terms of ΔV, the direct ascent launch strategy has not been adopted for Gaia.

To place the line of apsides into the direction of SEL2 and also close to the ecliptic plane independently of orientation of the Earth's axis, the nose module comprising Gaia and Fregat is initially injected into a circular parking orbit with 15° inclination and an altitude of about 180 km. This is the maximum inclination which still allows for a Gaia S/C mass of 2,100 kg. The drift duration in the parking orbit can theoretically be freely chosen, which allows to always select a launch time and argument of perigee to place the line of apses into the direction of SEL2 and close to the ecliptic plane and thus minimizing the effort for the insertion manoeuvre. An inclination of 23.5° would have been optimal with respect to balancing the ΔV, but the launcher performance in combination with range safety constraints would not have allowed to reach a sufficiently high apogee altitude.

4. Transfer Design with Constraint Spacecraft

After having discussed the orbit selection and the general transfer strategy this section will discuss the more detailed transfer strategy and launch window calculation, adding the initially assumed S/C constraints. The manoeuvres will be discussed sequentially. But prior to discussing the manoeuvres and their ΔV allocation the design of Gaia should be discussed, since it results in quite some constraints on the manoeuvres.

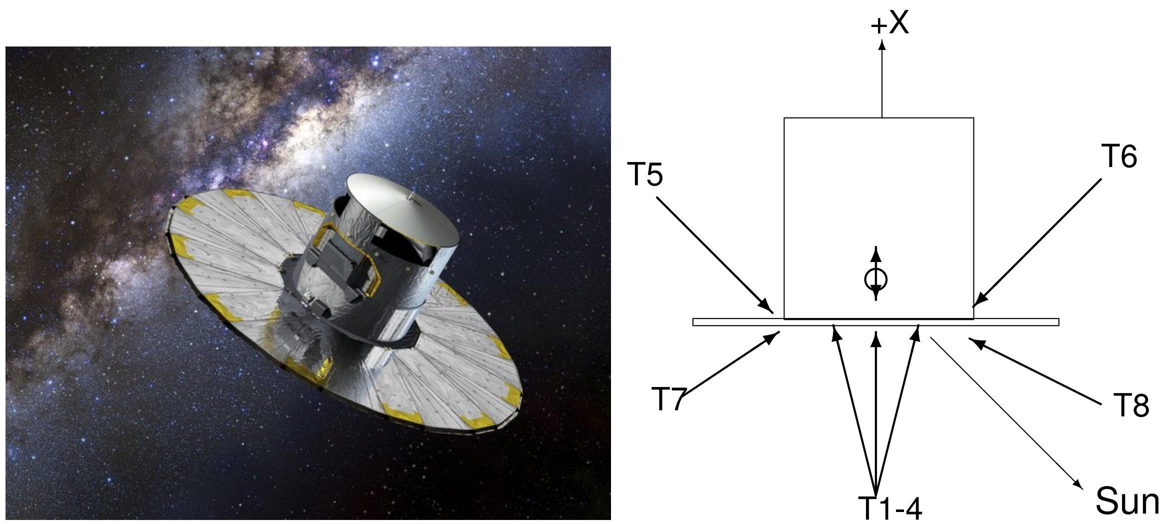

Figure 2. Gaia Spacecraft and schematic thruster layout. (Copyright ESA-D. Ducros, 2013)

Gaia, as shown in Fig. 2, has a large sun-shield and a cylindrical section, which contains the payload and service module covered by the thermal tent. The Sun may never be on the cylindrical section of the S/C with the exception of the launcher ascent, when the sunshield is still folded up and protects the payload and service module. The sunshield is deployed after the correct attitude with respect to the Sun has been acquired. The symmetry/rotation axis of Gaia must maintain a 45° angle to the Sun in order to keep the thermal balance. This constraint is active for the entire mission after the first transfer correction manoeuvre.

The thruster layout of Gaia is a further feature adding constraints. The schematic thrust vectors of the eight chemical propulsion system thrusters used for attitude and orbit control are also shown in Fig. 2. Thruster 1-4 all have a small angle with respect to the center of mass (CoM) and can thus provide torque control. Thruster 5+6 shall not be used to avoid payload contamination, but they can also not be used for a prolonged period of time, since the propellant would then settle towards the top of the S/C (+x direction) and it would not reach the tank outlet, which is in the opposite direction. They can be only be used for station-keeping manoeuvres of limited size.

A similar constraint exist for the utilization of Thruster 8. Unfortunately Thruster 8 cannot be replaced by Thruster 7 and a rotation of the S/C by 180° since the telescope openings shall be kept as far away from the Sun as possible during manoeuvres. In summary, thruster 1-4 + 7 shall be used for orbit manoeuvres only. The combination of attitude with respect to the Sun and thruster utilization constraints leads to the interesting fact that the S/C cannot be accelerated towards the Sun. The thrusters that can be used for a prolonged period of time are all on the illuminated side of the Sun shield and the S/C cannot be turned around.

4.1. The First Transfer Correction Manoeuvre

The first transfer correction manoeuvres serves two purposes, the correction of the launcher dispersion and the correction of the required apogee altitude. The ΔV required for the correction of the launcher dispersion is given by the required probability. Usually the 99.73% probability (3σ) is used. The definition of the length of the monthly launch window determines the second part of the ΔV allocation. To explain this we can make the simplified assumption that to achieve a ΔV optimal insertion manoeuvre we always have to target a similar state near the SEL2 point. This requires the S/C to have the correct apogee altitude. While the launcher always puts the S/C on the same trajectory departing Earth, the apogee altitude can be altered by third body perturbations. Since the transfer trajectory is close to the ecliptic plane it will at some point pass by the orbit of the moon. Dependant on the orbital phase of the moon Gaia will have a different distance from the moon and thus a more or less pronounced perturbation by it. This perturbation can either raise or lower the apogee value. Fig. 3 shows the required apogee altitude and corresponding perigee velocity at Earth departure to reach the optimal insertion point for the launch period end of 2013-begin of 2014.

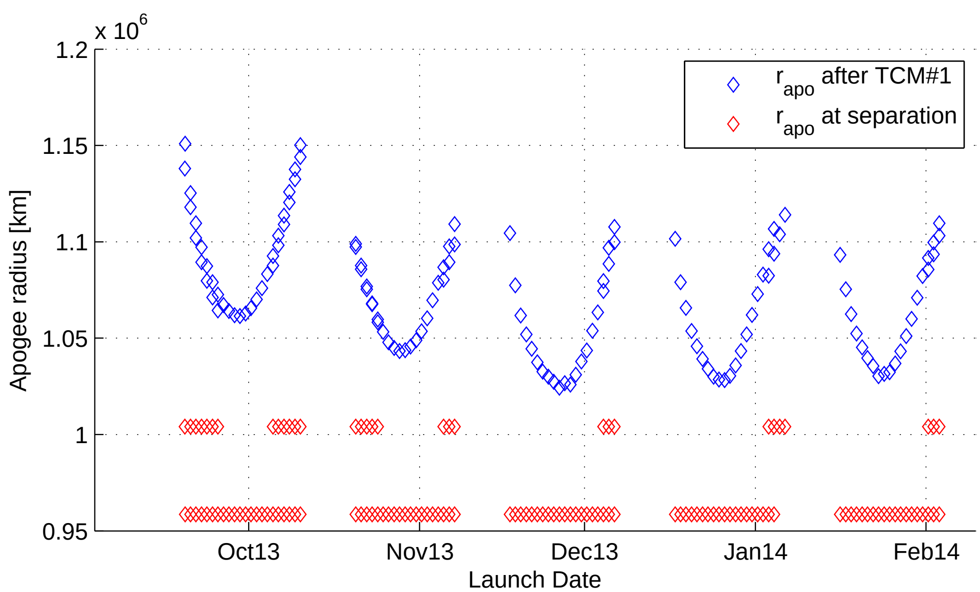

Figure 3. The required apogee altitude for the Gaia transfer is reached after the first transfer correction manoeuvre. The variation is due to lunar influence.

By defining the length of the monthly launch window the optimal perigee velocity plus the ΔV interval to be covered can be defined. Unfortunately there is another factor impacting the size of the first transfer correction manoeuvre: The time of execution. The later the manoeuvre is executed, the more expensive it will be. Fig. 4 shows the amplification factor on how much it costs to correct a deviation in the perigee velocity.

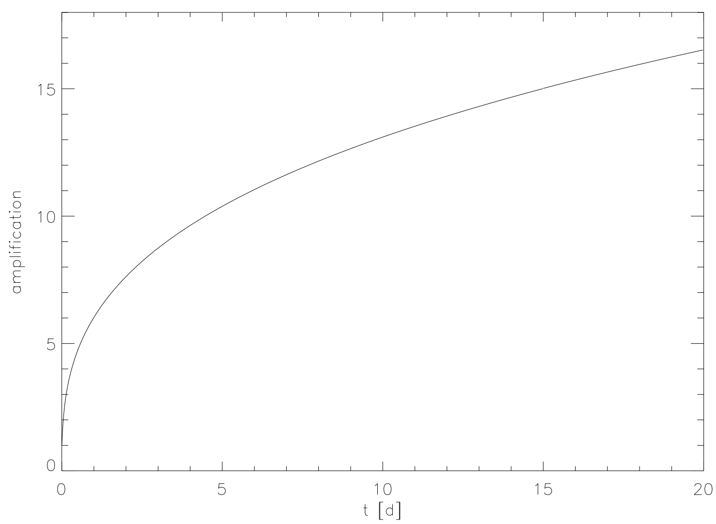

Figure 4. Amplification of the tangential velocity difference due to the dynamics on a parabolic escape trajectory.

As is can be seen it is desirable to correct the velocity as early as possible, but there are some limits. Firstly, the trajectory must be determined by radiometric measurement prior to calculating the actual manoeuvre and secondly the S/C might not be ready for a manoeuvre immediately after separation from the upper stage. Realistically the manoeuvre can be executed about 24 hours into the mission, however, to account for contingencies an execution on day-2 is assumed. As it can be seen from Fig. 4 any required correction in the perigee velocity will have grown by a factor of more than eight by then.

Regrettably this was not the last penalty factor to be added. Since the S/C cannot be accelerated towards the Sun, the initial apogee altitude targeted by the launcher must be biased such that the S/C can also deal with a launcher over-performance. In case of a launcher over-performance (which actually occurred on the Gaia launch), the S/C would need to accelerate towards the Sun in order to lower the apogee altitude. Due to the constraint above this is not possible. The Soyuz-Fregat thus injects the S/C into an orbit with a nominal apogee altitude lower than the optimal one. This can be clearly seen in Fig. 3, where the apogee altitude at separation is always lower than the actual required apogee altitude for the transfer. This means that even in case of a nominal launcher performance a manoeuvre must be executed and the S/C must be accelerated to the required apogee altitude. To still cover a possible under-performance of the S/C an even larger manoeuvre must be anticipated. The biasing of the apogee altitude adds another penalty factor of two to the budget of the first transfer correction manoeuvre.

In total this means that any deviation from the required perigee velocity on a specific launch day will have to be multiplied by a factor of more than 16 for the budgeting of the first transfer correction manoeuvre.

4.2. Second and Third Transfer Correction Manoeuvres

With a perfectly executed 1st transfer correction manoeuvre the S/C would in theory travel to the required location for the insertion manoeuvre. But firstly the manoeuvre cannot be perfectly executed, secondly there will be internal and external perturbation on the S/C which need to be corrected and thirdly the TCM#1 must also be slightly biased to ensure correct execution direction for TCM#2. TCM#3 is small enough to be also executed into the Sun direction and thus the second manoeuvre doesn't need to be biased anymore.

Those manoeuvre mainly depend on the perturbation environment and the manoeuvre execution error of the S/C. In flight the two additional manoeuvres were not required, the insertion point could be reached with sufficient accuracy after TCM#1 execution.

4.3. Insertion Manoeuvre

In an unconstrained transfer optimization to a small amplitude Lissajous orbit around SEL2 the optimal insertion manoeuvre will have a ΔV-to-Sun angle of about 90°. Due to the attitude constraint and thruster layout an efficient manoeuvre on Gaia can only be flown at ΔV-to-Sun angles larger than 100° utilizing the thruster combination 1-4 + 7. The insertion manoeuvres is the largest manoeuvre of the mission. After the successful execution of the manoeuvre the S/C is in its operational orbit around SEL2 once manoeuvre execution error have been corrected.

Since the insertion manoeuvre is also time critical the initial point for the insertion manoeuvre was placed such that an insertion was still possible with a delay of two days.

4.4. Station-Keeping Manoeuvre

Due to the inherent instability of orbits around SEL2 regular station-keeping manoeuvres are required. Those are only conducted when required, but a slot is allocated every 30 days. Due to the very well predictable perturbations on Gaia the station-keeping manoeuvres are rather small. The S/C must leave the scan law and change to an inertially fixed attitude, maintaining the 45° SAA. A reference orbit is not targeted with Gaia but merely the unstable component is removed from the motion. The manoeuvres are thus executed into the unstable direction (see Equ. 6).

4.5. Moon Eclipse Shortening Manoeuvre

Due to the size of the Lissajous orbit to be limited to less than 15° unfavourable conditions with respect to the moon can occur, where the moon is causing a partial eclipse for a prolonged period of time (up to 42 hours). While not problematic with respect to solar power generation it is undesirable with respect to the thermal balance. This situation is depicted in Fig. 5. A manoeuvre changing the shape of the SEL2 orbit can avoid this situation. In the final Gaia trajectory this situation could not occur anymore due to changed insertion conditions, which resulted in more favourable conditions with respect to the trajectory of the moon due to larger out-of-plane amplitudes.

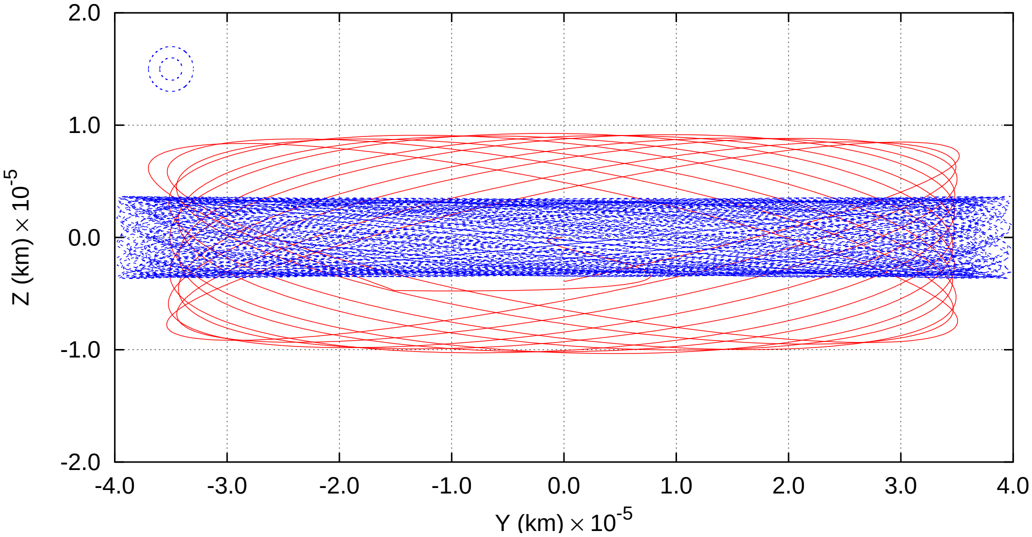

Figure 5. Trace of sample operational Gaia orbit and moon in YZ-plane at SEL_2 distance. The size of the penumbra and of the antumbra are shown in the upper left corner of the figure.

4.6. Earth Eclipse Avoidance

Any small amplitude Lissajous orbit about SEL2 will have an eclipse following the natural motion. By choosing appropriate initial conditions the time to an eclipse can usually be extended to 6.5 years for orbits with SSCE $\sim 15^\circ$, if appropriate initial phase angles are selected. Modifying these phase angles during the operational orbit can be used to ”jump” over an eclipse and restore the conditions for another long eclipse free period. The manoeuvre size to ”jump” in phase angle depends on the actual libration point orbit and by how much the phase needs to be adjusted. The in-plane phase or the out-of-plane phase can be adjusted. A description and comparison of different eclipse avoidance strategies can be found in [6].

4.7. Disposal

A disposal strategy has not yet been defined for Gaia, however, a heliocentric disposal seems to be the most likely option. The unstable component of the motion is excite in the direction of the solar system and the S/C will temporarily leave the Earth-Moon system on a trailing orbit. A return to Earth after several years cannot be excluded.

4.8. Manoeuvre Summary

Table 1 provides a summary of the anticipated manoeuvre sizes and manoeuvre directions for the Gaia transfer.

Man.		Circular 15 DEG	sun-ΔV angle
1	Launcher dispersion correction and perigee velocity correction (day 2)*	70 m/s	$\geq 135°$
2	Mid-course Corrections and navigation	20 m/s	any direction
3	Orbit Insertion*	165 m/s	110°-130°
4	Lunar Eclipse duration shortening	10 m/s	non-escape (within 5° from plane orthogonal to escape direction)
5	Orbit maintenance for 5.5 years mission lifetime	11 m/s	within 5° from escape direction = line in x-y plane 28.5° (208.5°)
6	Orbit maintenance for 1 years mission extension	2 m/s	within 5° from escape direction = line in x-y plane 28.5° (208.5°)
7	Eclipse avoidance manoeuvre for 1 year mission extension	0-15.1 m/s	in $\pm z$-direction of rotating frame
8 + 9	L2 Departure and Jacobi raising (both optional)	0.5-max. remaining	

Table 1. Geometric ΔV values for Gaia fast transfer. (* for the launch window calculation the single manoeuvres are allowed to exceed the allocated value as long as the sum of TCM#1 and the orbit insertion manoeuvre does not exceed the sum of the allocations.

5. Emerging Problems

The section above describes the baseline mission which leads to the construction of the S/C and the appropriate trajectory design. With evolving documentation of the spacecraft two major problems surfaced:

- The propellant allocation of the S/C did not support the specified manoeuvres
- The manoeuvre execution error was extremely high rendering the ΔV allocation for transfer navigation invalid

5.1. Mean Value vs. Mean Value - Solving the Propellant Allocation Problem

How can it happen that the propellant allocation does not match the ΔV specification? While the specification gives the so called geometric $\Delta V_{geometric}$, which is the impulsive change in velocity the S/C actually experience, the so called effective $\Delta V_{effective}$ is the ΔV related to propellant consumption through the Tsiolkovsky equation and contains all additional losses (e.g. gravity losses). The $\Delta V_{effective}$ can be significantly larger, e.g. if thrust decomposition is required to achieve a manoeuvre by two or more separate ones.

While the low efficiencies in some directions were known, some of the manoeuvre specifications required a manoeuvre in more than one direction, e.g. the station-keeping manoeuvre could be in the unstable direction pointing towards or away from the Sun. To calculate the propellant budget the mean efficiency of the manoeuvres was utilised, but the wrong mean had been calculated. In this calculation one cannot use the arithmetic mean, but must use the harmonic mean. If e.g. one manoeuvre has an efficiency of 100% and the second manoeuvre has an efficiency of only 50% the mean efficiency is not 75%, because the propellant consumption for 1 m/s in each direction is 1 m/s and 2 m/s for the manoeuvre with 100% and 50% efficiency, respectively. The resulting efficiency is 2 m/s / 3 m/s = 0.667, which is 66.7%. This is the harmonic mean, significantly lower than the arithmetic mean. The situation worsens with low efficiencies and some manoeuvre directions on Gaia had efficiencies of less than 30% (compare Fig. 6).

In this case the mitigation strategy consists of two parts. Firstly, a turn and burn strategy leaving the prescribed Sun aspect angle of 45°, which allowed an increase of the minimum manoeuvre efficiency to about 40% depicted by the green curve in Fig. 6. This low value is reached for absolute values of the ΔV-to-Sun angle near 70°. As it can be seen from the Figure, the increase in efficiency around this minimum is rather steep. Thus, in order to further raise the efficiency a simple manoeuvre decomposition was applied. Since the increase in efficiency is greater than the cosine losses by the manoeuvre decomposition the total efficiency increases. For example a manoeuvre planned at -70° ΔV-to-Sun angle, which provides the worst case in terms of efficiency can be replaced by two manoeuvres with ΔV-to-Sun angles -97° and -43°, resulting in an efficiency of more than 66% without margin. The maximum efficiency that can theoretically be reached for each ΔV-to-Sun direction by optimal combination of vectors using an asymmetric decomposition is also depicted in Fig. 6 by the black curve. The minimum efficiency is now above 55% and this already contains a margin of 5% to account for losses.

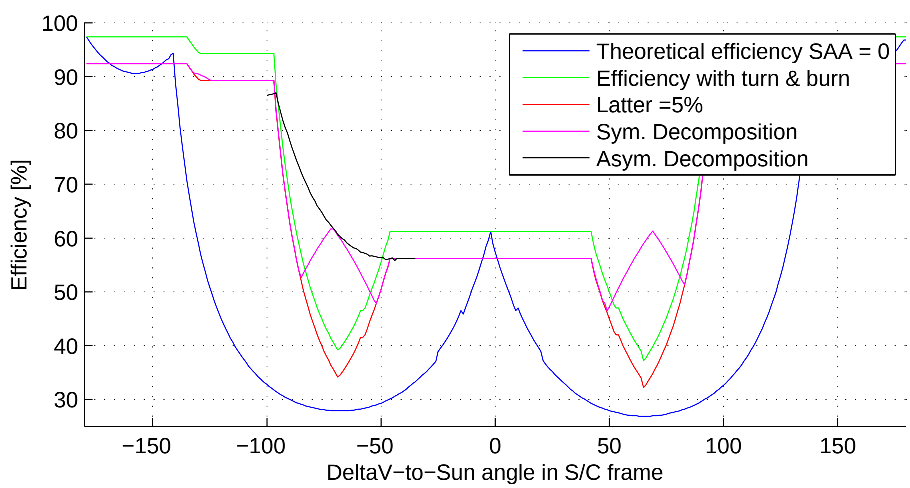

Figure 6. Manoeuvre efficiency dependant on ΔV-to-Sun angle for different manoeuvre strategies for the Gaia chemical propulsion system configuration and Sun aspect angles between 0-45°.

The minimum manoeuvre efficiency could be almost doubled and as a result a positive margin could be re-established on the propellant budget. The drawback of this strategy is a loss of the thermal balance because it requires to leave the SAA of 45° with respect to the Sun. If the strategy was to be applied this would result in a delayed start of the science phase due to the lacking thermal stability.

5.2. An Accurate Inaccurate System

The second problem was revealed from the chemical propulsion system performance report. The directional manoeuvre error is specified with respect to the desired manoeuvre direction in the S/C frame. The azimuth angle defining the manoeuvre direction is the angle of the ΔV from the +x-axis. The directional error with respect to the azimuth angle is provided in Fig. 7.

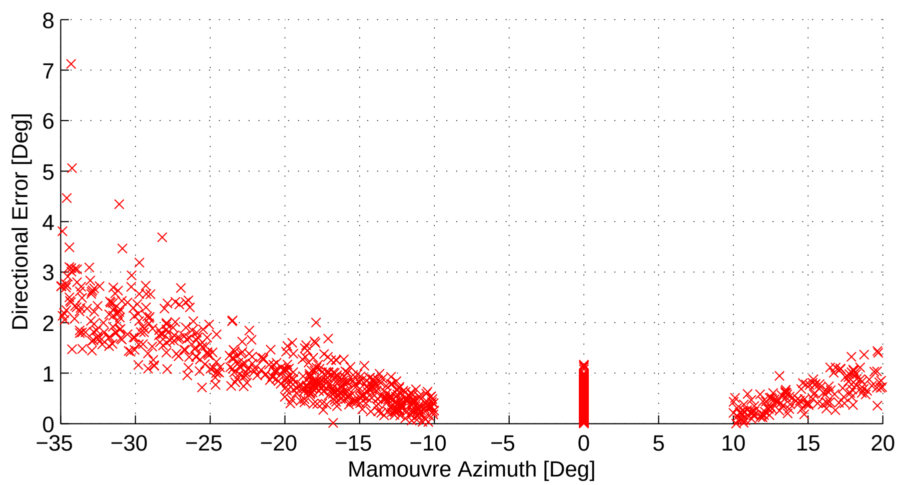

Figure 7. Gaia directional manoeuvre error with respect to manoeuvre azimuth.

The insertion and thus the largest manoeuvre was planned to be executed at an azimuth angle of -35°. Due to the SAA of 45° the x-axis has an angle of 135° with respect to the Sun. At an azimuth angle of -35° the ΔV-to-Sun angle is 100°. As it can be seen in Fig. 6 a high efficiency is achieved for such a ΔV-to-Sun angle. The report specified the directional error of the manoeuvre at the required ΔV-Sun-angle for the insertion manoeuvre to be more than 7°. When calculating the vector error of a manoeuvre with 165 m/s, the vector error could be as large as 20 m/s. And since a direction of this error had not been specified, it could have been into the anti-Sun direction, requiring an acceleration of the S/C into the Sun direction to compensate for this error. Since this is not possible by design, angular biasing could have been applied, requiring a total correction ΔV allocation of about 40 m/s, roughly 25% of the total manoeuvre, exceeding the already marginal propellant budget.

Again an averaging mistake had been made when characterizing and qualifying the system. The system was not characterized by the worst case performance within the given boundaries, but by the mean performance. The mean directional error had been calculated by taking the mean angular error of all simulation runs. Since the angular error is always positive the mean also had to be a positive value, even if the mean vector would have coincided with the required manoeuvre direction. Of course the system appeared to be rather accurate, since many of the runs were executed in an accurate direction, lowering the calculated (meaningless) standard deviation of the error.

With the S/C manufacturer unwilling to re-assess the performance of the system a detailed analysis of the available data was started to identify the cause of such a large directional error. A problem with the CoM position has already been identified by the manufacturer. For the simulation runs the CoM of each unit in the spacecraft model had been shifted randomly and an overall CoM had been calculated. This approach resulted in an unrealistic CoM distribution of the overall CoM value incompatible with the overall CoM limits. The CoM distribution and the box with valid CoMs are provided in Fig. 8.

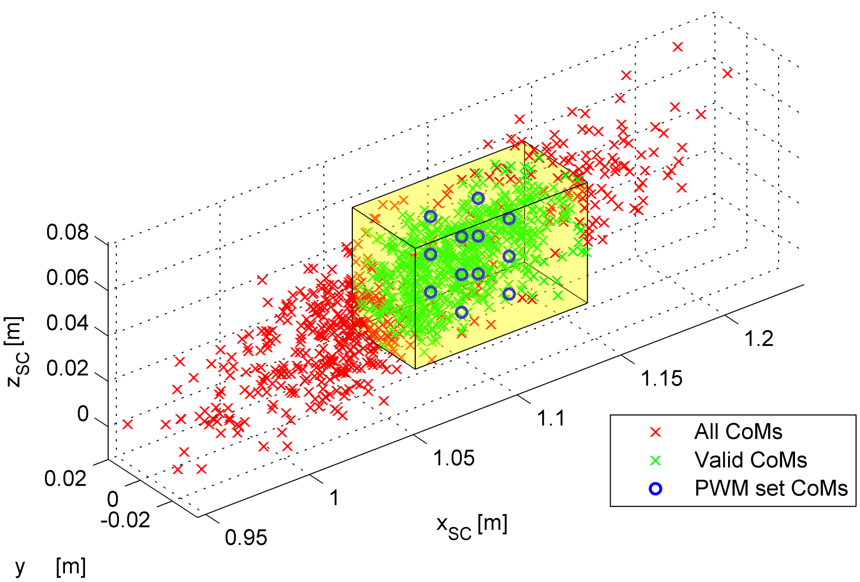

Figure 8. Gaia CoM distribution of the simulation runs to characterize the chemical propulsion system, the valid region of CoMs and the CoMs used in the Pulse Width Modulation (PWM) calculations use in the re-assesment.

Surprisingly, after pruning the unrealistic CoMs a large directional error remained. The next step was to look for correlations between the simulation input data and the angular error. Initially a correlation could not be found. While some of the runs with bad accuracy showed a large deviation of the CoM there were also runs with a CoM location close to the expected one, which also showed a bad directional accuracy. After some further investigations the problem could be tracked down to the two different CoM positions used in the simulation, the CoM of the S/C used in the specific simulation run and the assumed CoM in the controller. Whenever the real CoM was away from the assumed one, the thrusters would generate an additional torque, which had to be compensated by the system. In the other case the controller assumed a different CoM location and thus actuating the thruster such that the activation would cause little torque with the assumed CoM. But since the real CoM was different from the assumed one, "artificial" torque was generated by the system, which also needed to be compensated to maintain a stable S/C attitude.

6. Mitigation Strategies

But why does additional torque on the system cause such a bad directional accuracy? The reason is the unbalanced propulsion system, which uses thrusters 1-4 to generate the torque for attitude control. Thrusters 1-4 are in general thrusting along the longitudinal axis, with a slight offset to achieve a lever arm with respect to the CoM. This means, spoken simplified, whenever a torque is generated, either due to a real offset of the CoM or due to an artificial one by an offset CoM assumption in the controller, an additional ΔV in the direction of the longitudinal axis will be generated. This behaviour was now investigated in a detailed simulation campaign together with the Gaia flight control team and the additional ΔV component could be characterised. On the one hand this was really good news, since the main part of the perturbing acceleration was identified to be acting in a pre-defined direction. On the other hand this was really problematic, since the additionally generated ΔV was exactly in the direction that cannot be compensated due to the limitations on the use of thrusters 5+6. It also meant that a ΔV-to-Sun angle of $100°$ was not achievable, since the additional component would always increase the ΔV-to-Sun angle.

Due to contractual reasons the characterization of the manoeuvre error by ESOC could not be used. It was thus required to find an alternative mitigation strategy. To control the manoeuvre directional error, a direction for the manoeuvre closer to the x-axis of th S/C was chosen. This required to limit the ΔV-to-Sun angle to $125°$, equivalent with an azimuth angle of $-10°$, which is sub-optimal with respect to ΔV, but optimal with respect to the manoeuvre accuracy (see Fig. 7).

Since now the additional ΔV component is only $10°$ from the desired one, the angular deviation is less severe, but is still there (compare Fig. 7). In order to allow for a correction within the given constraints, the manoeuvre was now not executed in one go, but split into two parts of 80% and 20%. This split was found to be sufficient to ensure that the second part of the manoeuvre was still within the efficient and accurate range. Nevertheless all this required additional ΔV with respect to the original baseline strategy.

The easy solution would have been to fill up the tanks of Gaia, since margin in the tank size had been specified and the launcher still showed some margin with respect to the current maximum wet mass of Gaia. Unfortunately this easy option could not be implemented, since the qualification test of the Gaia structure had been performed with the nominal propellant load and an increase in the wet mass would have rendered the qualification test invalid.

Thus the S/C would not offer additional ΔV and the launch window calculations had to be adapted. A different strategy was chosen making optimal use of the two available Fregat flight programs (FP). The additional ΔV would theoretically shorten the monthly launch window. This shortening could be recovered by a benign launch season and utilizing the second FP not with a different argument of perigee in order to extend the launch season, but with a different apogee radius to recover the monthly launch window.

Around the winter solstice the optimal argument of perigee changes very slowly from day to day and a flight program with an average argument of perigee value can not only be used for the month the value is valid, but also for a large part of the pervious and next month. The second available flight program was thus not used to cover a different launch month with a different argument of perigee. It was used with the same argument of perigee as the first, but the apogee radius/perigee velocity was selected differently in order to have the launch vehicle perform the now missing ΔV on the S/C. This change in the apogee radius can be seen in the nominal separation apogee altitude shown in Fig. 3. By optimizing the argument of perigee and the apogee altitude of both flight programs a launch period of about four months could be covered with gaps in the launch window of 10-12 days per month.

7. Conclusion

At a very late stage in the Gaia project two significant problems were discovered: An insufficient propellant allocation due to a mistake in the manoeuvre efficiency calculation and an unacceptable large directional manoeuvre execution error. Both problems had to be accounted for in the trajectory design, since a useful characterisation of the manoeuvre error and re-qualification of the S/C structure were to be avoided. The solutions found to the problem consisted of manoeuvre decomposition for suboptimal directions and a complete re-design of the transfer trajectory, adjusting the Fregat FPs to deal with the increased ΔV demand, enforcing more accurate manoeuvre directions and splitting the manoeuvres such that a correction would be possible.

In the end a feasible mission design could be recovered, proving the value of strong mission analysis involvement in phase C/D/E.

Lessons learned:

- Mission Analysis involvement in phase C/D/E
- Be sure to think through specific design solutions (mounting of thruster 7) to allow for them to be effective

Gaia was successfully launched on the 19th of December at 9:12:19 UTC. The S/C arrived in its operational orbit on the 15th of January 2014 after execution of the 2nd part of the orbit insertion manoeuvre. Prior to the execution of the insertion manoeuvre a calibration burn had been performed to even better characterise the system performance.

8. References

[1] Gomez, G., Masdemont, J. J., and Mondelo, J. M. “Libration Point Orbits: a Survey from a Dynamical Point of View.” “Libration Point Orbits and Applications,” World Scientific Pub Co., 2003.

[2] Cobos, J. and Masdemont, J. J. “Astrodynamical Applications of Invariant Manifolds Associated with Collinear Lissajous Libration Points.” “Libration Point Orbits and Applications,” World Scientific Pub Co., 2003.

[3] Farquhar, R. W. The Control and use of Libration-Point Satellites. TR-R 346. NASA, 1970.

[4] Szebehely, V. Therory of Orbits. Academic Press, New York, 1967.

[5] Hechler, M. and Yánez, A. "Herschel/Planck Consolidated Report on Mission Analysis Issue 3.1." Tech. Rep. PT-MA-RP-0010-OPS-GMA, European Space Operations Centre (ESOC), Darmstadt, 2006.

[6] Renk, F. "Mission Analysis for Exploration Missions Utilizing Near-Earth Libration Points." PhD Thesis, Insititute of Space Systems, University of Stuttgart, October 2009.

[7] Hechler, M. and Cobos, J. "FIRST Mission Analysis: Transfers to Small Lissajous Orbits around L_2." MAS Working Paper 398, Mission Analysis Section, ESA/ESOC, July 1997.

[8] Howell, K. C. "Families of Orbits in the Vicinity of the Collinear Libration Points." Tech. rep., The Journal of Astronautical Sciences, Vol. 49, No. 1, pp. 107-125, 2001.